

1 The Chromosome-based Genome of *Paspalum vaginatum*

2 Provides New Insights into Salt-stress Adaptation

3 Li Liao^{1,4}, Xu Hu^{1,4}, Jiangshan Hao^{1,4}, Minqiang Tang^{2,4}, Longzhou Ren¹, Ling Pan²,
4 Shangqian Xie², Paul Raymer³, Peng Qi³, Zhenbang Chen³, Zhiyong Wang² & Jie
5 Luo¹

6

7

7 1 College of Tropical Crop, Hainan University, Haikou 570228, China

8 2 College of Forestry, Hainan University, Haikou 570228, China

9 3 Department of Crop and Soil Science, University of Georgia, Griffin, GA 30223

10 4 Author contributed equally to this work

11

12 Corresponding author

13 Correspondence to: Zhenbang Chen (zchen@uga.edu)

14 Zhiyong Wang (wangzhiyong@hainanu.edu.cn)

15 Jie Luo (jie.luo@hainanu.edu.cn)

16

17 Abstract

18 Salinization is increasingly a major factor limiting production worldwide. Revealing
19 the mechanism of salt tolerance could help to create salt-tolerant crops and improve
20 their yields. We reported a chromosome-scale genome sequence of the halophyte
21 turfgrass *Paspalum vaginatum*, and provided structural evidence that it shared a
22 common ancestor with *Z. mays* and *S. bicolor*. A total of 107 *P. vaginatum*
23 germplasms were divided into two groups (China and foreign group) based on the
24 re-sequenced data, and the grouping findings were consistent with the geographical

25 origin. Genome-wide association study (GWAS) of visually scored wilting degree and
26 withering rates identified highly significant QTL on chromosome 6. Combination with
27 RNA-seq, we identified a significantly up-regulated gene under salt stress, which
28 encodes ‘High-affinity K⁺ Transporter 7’ (*PvHKT7*), as strong candidates underlying
29 the QTL. Overexpression of this gene in *Arabidopsis thaliana* significantly enhanced
30 salt tolerance by increasing K⁺ absorption. This study adds new insights into salt-stress
31 adaptation of *P. vaginatum* and serve as a resource for salt-tolerant improvement of
32 grain crops.

33

34 **Keywords: Seashore paspalum, Genome assembly, Population genetics, GWAS,**
35 **Salt tolerance**

36

37

38 **Introduction**

39 Salinization is increasingly a major factor limiting production worldwide. Saline
40 alkali land accounts for 2.1% of the world's total land and as much as 19.5% of
41 irrigated land (www.fao.org/soils-portal). Most of the crops are salt-sensitive, which
42 inhibits seedling growth and decreases yields when growing in salt-affected soils(Roy
43 et al., 2014; Farooq et al., 2015; Acosta-Motos et al., 2017). Therefore, in the areas that
44 have been already salt-affected or vulnerable to salinization because of seawater
45 intrusion or storm surges, the development of salt-tolerant varieties is a very critical
46 target.

47 Seashore paspalum (*Paspalum vaginatum*) has been utilized as turf for almost one
48 hundred years(Wu et al., 2018; Qi et al., 2019) and the species is largely diploid
49 (2n=2x=20). *P. vaginatum* is an important halophytic warm-seasoned perennial grass
50 widely used on athletic fields, golf courses, and landscape areas in tropical and
51 subtropical regions. It can be propagated rapidly by stolons and rhizomes to form a
52 fine-textured turf(Liu et al., 2017; Wu et al., 2020). Owing to its tolerance to abiotic
53 stresses, and its ecological aggressiveness, it is not only widely used as a turfgrass, but
54 also serves as forage and ground cover for reducing erosion(Liu et al., 2017). *P.*
55 *vaginatum* has strong salt tolerance and can even be watered with seawater for short
56 periods making it especially important in locations near the sea or regions with water
57 quality issues.

58 Because of the wide geographic distribution and long-term effects of natural or
59 artificial selection, there are a number of diverse varieties for *P. vaginatum*, but only
60 few genetic resources are currently available. For years, relevant studies have mainly
61 focused on diversity analyses using random amplified polymorphic DNA (RAPD)
62 markers(Liu et al., 1994), amplified fragment length polymorphisms (AFLPs)(Chen et

63 al., 2005), and simple sequence repeat (SSR) markers(Shen et al., 2020), in attempts to
64 identify loci associated with salt tolerance traits (Wu et al., 2018) or dollar spot
65 resistance traits(Catching et al., 2019). A high-density genetic map of *P. vaginatum*
66 indicated *P. vaginatum* is closely related to the important grain crops such as maize,
67 sorghum and millets(Qi et al., 2019). Hence, greater understanding of the molecular
68 mechanisms of *P. vaginatum* salt tolerance may provide a gateway opportunity to
69 improve salt tolerance in cereal crops. Simultaneously it could be contributed as a
70 model to the study of salt tolerance in grasses.

71 Here, we integrated Pacbio, Hi-C, RNAseq, Illumina short reads, and 10 ×
72 Genomics data, presenting a chromosome-scale assembly genome of *P. vaginatum*
73 ‘SeaIsle2000’, a cultivar with high turf quality introduced to South China several years
74 ago. To better understand the genetic basis of salt tolerance traits in *P. vaginatum*, we
75 re-sequenced 107 accessions collected globally. By conducting a genome-wide
76 association study (GWAS) and molecular experiment, we identified several QTLs and
77 verified the *PvHKT7* gene related to salt resistance in *P. vaginatum*. Together, this
78 study provided a foundation for accelerating the genetic improvement of *P. vaginatum*,
79 furthermore this genetic resource may potentially be used for salt tolerance research
80 and biotechnology assisted improvement of other grasses as well as other crops.

81 **Results**

82 **Chromosome-scale Genome Sequencing and Assembly**

83 A diploid cultivated *P. vaginatum*, SeaIsle2000, planted widely with high turf
84 quality, was selected for genome sequencing, using four sequencing and assembly
85 technologies: Illumina short-read sequencing, PacBio long-read sequencing, 10 ×
86 Genomics and Hi-C data (Table S1). The genome size was estimated to be 589.20 Mb

87 based on K-mer analysis (Fig. S1a) and flow cytometry analysis (Fig. S1b), close to the
88 600 Mb reported by previous estimates(Eudy et al., 2017). Primary genome contigs of
89 *P. vaginatum* were produced by PacBio (~94.90×). Then, we used Illumina reads
90 (~100.62×) to perform sequence error correction of contigs. The consensus sequences
91 were further scaffolded by integrating with 10× genomics linked reads (~92.52×). The
92 assembly V1 consists of 185 scaffolds, and its contig N50 was up to 5.46 Mb while its
93 scaffold N50 was 9.06 Mb (Table S2). We plotted the distribution of GC content and
94 sequence depth by 10 kb slide window and found that this assembly had no GC bias and
95 was polluted (Fig. S2). Finally, in order to improve the quality of assembly, 64.15 GB
96 Hi-C clean reads were used to assist the assembly correction and mapped to raw
97 genome assembly. After filtering those unmapped and duplicative reads, 117 scaffolds
98 were clustered and ordered into 10 pseudo-chromosomes (Fig. S3), with a
99 super-scaffold N50 of 47.06 Mb (Table S2, assembly V2).

100 The final *P. vaginatum* assembly captured 517.98 Mb of genome sequence,
101 consisting of 10 chromosomes and 169 scaffolds (Table S2), with 485.64 Mb (~93.76%)
102 anchored into chromosomes (Table 1). We identified 1572 (97.40%) of the 1614
103 conserved genes with BUSCO and 239 (96.37%) of the 248 core eukaryotic genes with
104 CEGMA in the genome assembly (Table S3). We found that 99.19% of the Illumina
105 short reads mapped to the Sealsle2000 genome. Furthermore, we used the 4078 SNP
106 markers that were mapped on the first available published integrated genetic linkage
107 map, the maternal parent map (HA map), the paternal parent map (AH map) and the
108 both parents map (HH map), to validate scaffold assembly. 1854 markers (98.36%),
109 1637 markers (98.97%) and 1276 markers (98.91%) were hit on the HA map, AH map,
110 and HH map, respectively (Table S4). Every linkage group largely corresponded to a

111 single SeaIsle2000 chromosome, such as HA genetic map, but some chromosomes
112 were completely inverted, such as chromosomes 2, 4, 5, 6 and 10 (Fig. S4). This
113 showed that the chromosome sequences of the assembly are coincident with previous
114 linkage groups. Taken together, these results suggest that the SeaIsle2000 genome is a
115 high-quality assembly.

116 **Genome Annotation**

117 Based on de novo and homology-based predictions and transcriptome data, a total
118 of 28,712 protein-coding genes were predicted, with an average coding sequence length
119 of 3.53 kb and an average of 4.99 exons per gene, its gene structure was similarly to the
120 common species, such as *A. thaliana*, *S. bicolor* and *Z. mays* (Table S5). Of the
121 28,712 predicted genes, 27,536 (95.90%) could be matched in at least one public
122 protein database and given function descriptions (Table S6). As expected, gene density
123 was higher on the arms than in the middle of the chromosomes (centromere regions)
124 (Fig. 1a).

125 There were 2,725 non-coding RNAs (555 miRNAs, 603 tRNAs, 331 rRNAs and
126 1236 snRNAs) predicted in the SeaIsle2000 genome sequence with a total length of
127 362.71 kb (Table S7). Curated repeat libraries and *de novo* prediction were used to
128 annotate the repetitive elements. A total of 474,904 repetitive elements were
129 identified, of which, 114,750 were tandem repeat elements with a mean length of
130 336.71 bp (Table S8).

131 **Comparative Genomic and Evolutionary Analysis**

132 We applied the predicted proteomes of *P. vaginatum* and 9 other sequenced
133 species to identify putative orthologous gene clusters. A total of 31,619 orthologous
134 gene families composed of 338,128 genes were identified from 10 plant species of
135 which, 6,949 clusters of genes were shared by the 10 species. 1800 (25.9%) of the

136 shared gene clusters were single-copy families (Fig. 1b). Further, 11,939 gene
137 families were present across *P. vaginatum*, *S. bicolor*, *O. sativa*, *S. italica* and *A.*
138 *tauschii*. Compared with these four plant species, *P. vaginatum* genome contained 436
139 specific gene families containing 849 genes (Fig. 1c; Table S9). Gene Ontology (GO)
140 term enrichment analyses of *P. vaginatum* specific genes showed that the cellular
141 component termed ‘cytoplasmic stress granule’ was enriched; ‘cellular response to
142 light intensity’, ‘cellular response to UV’ and ‘root hair elongation’ were enriched in
143 the biological process categories (Fig. 2a; Table S10) which may be adapted to
144 tropical climates in *P. vaginatum*. KEGG pathway enrichment analyses of *P.*
145 *vaginatum* specific genes showed that ‘Linoleic acid metabolism’, ‘Flavonoid
146 biosynthesis’ and ‘MAPK signaling pathway’, etc. were significantly enriched (Fig. 2b;
147 Table S10) which may contribute to the special characteristic of salt-resistant in *P.*
148 *vaginatum*.

149 A set of single-copy ortholog genes of the 10 plant species that included 8
150 monocots and 2 eudicots, and applied to construct a phylogenetic tree. Phylogenetic
151 tree revealed *A. thaliana* and *M. truncatula* were clustered in one branch, *B. distachyon*,
152 *H. vulgare*, *A. tauschii* and *O. sativa* were clustered in one branch, *S. italica*, *S. bicolor*,
153 *Zea mays* and *P. vaginatum* were clustered in the other branch (Fig. 1d). These
154 topologies of these species were consistent with the results of published papers. The
155 divergence time between the monocots and eudicots were estimated to be 138.2-190.0
156 million years ago (Ma) (95% confidence interval). The tree indicated that *P.*
157 *vaginatum*, *S. bicolor* and *Z. mays* might share a common ancestor and their
158 divergence time was estimated to be about 23.7 Ma (the interval was 21.1-26.8 Ma).

159 According to the close relationship of *P. vaginatum*, *S. bicolor* and *Z. mays*, we
160 investigated the whole-genome duplication (WGD) events during the evolutionary

161 course of the 3 species. A total of 2,123 gene pairs were identified as segmental
162 duplications in ten chromosomes of the *P. vaginatum* genome (Table S11). Among
163 these gene pairs, 318 (14.98%) were located on the same chromosome, the others
164 were across different chromosomes. The widespread gene duplications suggested that
165 a WGD might have occurred during *P. vaginatum* genome evolution. Based on the
166 previous research, there is a very well synteny gene between *P. vaginatum* and *S.*
167 *bicolor*. Here, more than half (60.45%) of the predicted *P. vaginatum* genes were
168 identified as synteny genes with *S. bicolor* genes, resulting in total 22,345 pair genes
169 (Fig. 3a; Table S12). The synteny analysis between the two genomes provided clear
170 structural evidence of a common ancestor. Further, we investigated the collinearity
171 between *P. vaginatum* and *Z. mays*, the results showed that 16,046 *P. vaginatum*
172 genes had good collinearity with *Z. mays* genes. Interestingly, many *P. vaginatum*
173 genes have one-versus-four synteny genes to *Z. mays* (Fig. 3b). The above results
174 indicated that *P. vaginatum*, *S. bicolor*, and *Z. mays* might share a common ancestor,
175 and *Z. mays* may have experienced two WGD events when compared with *P.*
176 *vaginatum* (Fig. 3c).

177 **Population structure and genomic variation**

178 To explore genetic variation in *P. vaginatum*, we re-sequenced 107 germplasms
179 with an average depth of 12.78× and 98.12% mapping rate of the Sealsle2000
180 genome (Table S13). Using this dataset, we identified 3,083,910 high-quality SNPs and
181 1,023,374 InDels, corresponding to 6.35 SNPs and 2.11 InDels per kb (Table S14). A
182 total of 68,402 SNPs (1.83%) and 19,196 InDels (1.45%) were located in gene coding
183 regions (Table S15). Next, we investigated the genetic structure of the *P. vaginatum*

184 population for clusters (K) from 2 to 10 based on 3.08 million SNPs. Delta K showed a
185 peak at 2 (Fig. S5), suggesting two clusters as the most appropriate option. This
186 supports the reliable result of two major discrete clusters of China and other countries
187 from population the phylogenetic tree and PCA (Fig. 4). But several germplasms were
188 not well separated into two populations, indicating the occurrence of genetic diversity
189 along with their adaptation to different environments. The China population of *P.*
190 *vaginatum* had higher nucleotide diversity ($\pi=2.04\times10^{-3}$) than the Foreign population
191 ($\pi=1.06\times10^{-3}$; Fig. S16). However, linkage disequilibrium (LD) decayed faster in the
192 Foreign population than in China population (Fig. S6). Tajima's D results of all
193 germplasms was 1.86, while it was 2.67 and 1.55 in China and the other countries
194 group, respectively, when all accessions were separated into different groups. This
195 indicates that there are more alleles of high/medium frequencies in the population due
196 to equilibrium selection and bottleneck effects. These results revealed that the allelic
197 diversity in the China population was higher than that in the other countries population.
198 FST between the two populations (FST = 0.37) demonstrated relatively higher genetic
199 distance (Table S16).

200 **Population phenotypic variation under salt stress**

201 The symptoms of plant leaves were observed and recorded under salt stress. We
202 used two criteria, wilting degree (WD3, WD7) and withering rates (WR3, WR7), to
203 estimate salt tolerance levels when evaluating the salt tolerance among 77 samples. The
204 descriptive statistics of WC and WR are provided in Table S17 and the distribution for

205 each trait is shown in [Fig. S7a](#). The variable coefficients of WD3 and WD7 were
206 69.95% and 20.65%, respectively, and variable coefficients of WR3 and WR7 were
207 51.06% and 43.13%, respectively. These results indicated that a wide range of
208 phenotypic variation among *P. vaginatum* germplasms were associated with salinity
209 tolerance. The correlations between growth response and stress were obviously positive
210 (0.33 to 0.80) and WR3 was highly correlated with WR7 (0.80). Furthermore,
211 correlation analysis ([Fig. S7b](#)) showed that these 4 traits were significantly correlated
212 with each other. We therefore adopted all of the traits as a meaningful indicator of salt
213 tolerance.

214 **GWAS for salt tolerance**

215 To identify candidate genes related to salt stress, annotations of the genes were
216 analyzed within the identified loci (10.9 kb up and down stream of the most significant
217 SNP), the *P*-value thresholds were set at 1.69×10^{-7} (significant, $0.5/n, -\log_{10}(P) = 6.77$)
218 and 1×10^{-6} (suggestive, $-\log_{10}(P) = 6$). Totally, 19 SNPs associated with resistance to
219 salt were identified and 26 candidate genes were detected. Manhattan and QQ plot of
220 GWAS results were shown in [Fig. S9](#). These candidate genes distributed on
221 chromosomes 3, 6, 9 and 10, with detailed information of the genes listed in [Table S18](#).
222 GO enrichment analysis was carried out to elucidate the specific biological functions of
223 the 26 candidate genes. The significantly enriched GO terms concerning sodium ion
224 transmembrane transport (GO:0035725), monovalent inorganic cation transport
225 (GO:0015672), cation transmembrane transport (GO:0098655) etc ([Table S19](#)).
226 Interestingly, a peak strongly associated with salt tolerance ([Fig. 5a;5b](#)), identified on
227 chromosome 6, was located in emOS140.194 (*PvHKT7*), which was the orthologous

228 gene with *HKT7*, a high-affinity potassium transporter in the *S. bicolor* genome. Five
229 SNPs with the lowest P values on *PvHKT7* gene generated two haplotypes (Fig. 5c).
230 And the five SNPs significantly associated with salt tolerance traits explained 46.98% ~
231 55.74% of the phenotypic variance (Table S20). The accessions with *PvHKT7*-Hap2
232 have better salt tolerance ($P < 0.05$) than those with *PvHKT7*-Hap1 (Fig. 5d).

233 **Selective sweep signals during salt tolerance improvement**

234 We divided *P. vaginatum* in this study into two population, high salt tolerance
235 population (ST) and salt sensitive population (SS) based on their phenotypes after salt
236 stress. The nucleotide diversity (π) of the SS (1.85×10^{-3}) was higher than ST ($1.40 \times$
237 10^{-3}), which indicated salt tolerance may be subject to similar selection in the course
238 of evolution. To detect selective sweeps driven by salt environment, we compared
239 genomic variations with high fixation index (FST) and reduction of diversity (ROD)
240 between the ST and SS. Above the dashed horizontal thresholds of top 5%, we
241 identified 478 overlapping sweeps between ST and SS containing 622 putative genes
242 (Table S21). GO enrichment analysis revealed that genes in the FST and ROD
243 overlapping were enriched in two groups of GO classifications (MF and BP),
244 including potassium ion transmembrane transporter activity (GO:0015079), metal ion
245 transmembrane transporter activity (GO:0046873) and xyloglucan metabolic process
246 (GO:0010411) etc. (Fig. S8; Table S22).

247 **Transcriptome analysis and genetic authentication**

248 To identify differentially expressed salt-tolerance related genes, we collected roots
249 and leaves from accession grin_UPG145 (salt tolerance accession) at 5 time points
250 under salt stress. The highest number of differentially expressed genes (DEGs) (Fig.
251 S10) was detected in leaves at 12 h after salt stress, with 3379 up- and 3460
252 down-regulated genes. The lowest number of DEGs occurred in roots at 5D, when only

253 3,866 genes were differentially expressed.

254 Furthermore, putative *HKT* genes were found by BLASTP in *P. vaginatum*. A total
255 of 6 candidate members in *P. vaginatum* were scanned on the basis of hidden Markov
256 model (HMM) search (Fig. S11a). There are up-regulated, down-regulated, or even no
257 difference in all *HKT* genes. But only *PvHKT7* was significantly up-regulated in every
258 treatment group compared to the control group (Fig. S11b), indicating that *PvHKT7*
259 gene plays a more important role under salt stress. Finally, we demonstrated the
260 function of the *PvHKT7* gene in transgenic *A. thaliana* which was not harboring a
261 *HKT7* gene itself. Three independent transgenic lines with high expression levels of
262 *PvHKT7* (Line1, Line2, Line3) and a non-transgenic (WT) line were selected for salt
263 tolerance evaluation. To test the effect of *PvHKT7* overexpression on salt tolerance,
264 3-week-old plants of Line1, Line2, and Line4 were exposed to 32 ds·m⁻¹ NaCl and 1/2
265 MS medium for 10 days. The results showed that biomass weight of transgenic plants
266 was significantly greater than that of WT under the salt treatment (Fig. 6). The root
267 length of transgenic plants was longer than WT in both two type mediums. The K⁺
268 content in leaves and roots of transgenic plants was significantly higher than that of
269 WT under salt treatment. These results indicated that *PvHKT7* gene enhanced salt
270 tolerance of plants by enhancing K⁺ absorption. These results indicating
271 overexpression of *PvHKT7* increased salt tolerance.

272 **Discussion**

273 *P. vaginatum* is an exceptionally salt tolerant grass species that inhabits warm,
274 coastal areas worldwide. Its ability to thrive in saline environments makes it a vital
275 resource that could contribute as a model to the study of salt tolerance in the grasses,
276 and as a potential source of salt tolerance genes that could be used to improve the salt
277 tolerance of other species. However, genetic studies of *P. vaginatum* are limited by

278 relatively few genomic resources. A highly continuous and complete reference genome
279 is essential for a wide range of population genetics studies and experimental research.
280 We selected the worldwide major cultivar SealsIle2000 for *de novo* sequencing and
281 assembled the reference genome. By combining four sequencing and assembly
282 technologies, we proposed a high-quality chromosome-scale assembly genome with
283 the high continuity and integrity. The SeaIle2000 reference genome size was 517.98
284 Mb, including 10 chromosomes and 169 scaffolds. We evaluated the consistency and
285 syntenic sequences with the first available published genetic maps of *P. vaginatum* and
286 showed our chromosome assembly had good collinearity when compared with
287 previous linkage groups.

288 Comparative analyses showed that *P. vaginatum* has a close genetic relationship
289 with many grain and forage producing members of the Panicoideae, such as *S. bicolor*
290 and *S. italica*. Comparative analyses showed that each seashore paspalum chromosome
291 was syntenic to and highly colinear with a single sorghum chromosome. The synteny
292 analysis indicated that *P. vaginatum*, *S. bicolor*, and *Z. mays* may share a common
293 ancestor, but there was various salt tolerance among them. *P. vaginatum* is a salt
294 tolerant grass which has an impressive level of salt tolerance and experiences its
295 greatest productivity under salt exposure of $\sim 15 \text{ dS m}^{-1}$, is self-incompatible so
296 individuals are obligate out-crossers and highly heterozygous⁴. Sorghum is believed to
297 tolerate soil and water salinity up to 6.8 and 4.5 dS m^{-1} of electrical conductivity,
298 respectively. Above these thresholds, a 16% yield reduction is expected per each soil
299 salinity unit increase(Calone et al., 2020). Maize is moderately sensitive to salt stress
300 and soil salinity is a serious threat to its production worldwide(Farooq et al., 2015).
301 The genetic loci in seashore paspalum that confers salt tolerance can be leveraged in
302 these important relatives in the future.

303 GWAS results identified several target regions that putatively control salt tolerance.
304 Both GWAS and transcriptomes showed that *HKT7* gene was particularly important for
305 salt tolerance in *P. vaginatum*, and the overexpression of *HKT7* increased the salt
306 tolerance of *A. thaliana*. *HKT7* was not found in *A. thaliana*, which indicated that the
307 transgenic *A. thaliana* of *HKT7* could enhanced the salt tolerance. *HKT7* is an example
308 of the value that target gene identification can bring to future functional studies and
309 molecular breeding. Our overarching goal in undertaking this research was to expand
310 our understanding of seashore paspalum and to identify salt tolerance candidate genes
311 that could be put forward for further characterization. Moreover, these data and
312 information are valuable resources for *P. vaginatum* research and breeding, and for
313 comparative genomic analysis of Poaceae species.

314 **Methods**

315 **Sample collection**

316 A total of 107 *P. vaginatum* accessions or cultivar genotypes with variation in
317 morphological characteristics and geographic origin were used in this study including
318 24 germplasm resources collected from south China and 83 germplasm resources
319 from United States stored in the USDA Plant Genetic Resources Conservation Unit
320 (USDA-PCGRU) and the University of Georgia (UGA). Detailed information about
321 the country of origin and ecotype for each accession is shown in [Table S13](#). The world
322 map showing origin information ([Fig. 4a](#)) was made using the R package
323 `ggplot2`(Wickham, 2016). All materials are preserved as germplasm resources of *P.*
324 *vaginatum* at the experimental field of Danzhou campus of Hainan University (N:
325 19°30'15.63"; E: 109°29'12.70"), which were respectively planted in 1 m × 1 m plots.

326 **Genome sequencing and assembly**

327 Genomic DNA extracted from young leaves of ‘Seaside2000’ were sent to
328 Metware Metabolic Technology (Wuhan, China) for library construction and
329 sequencing by Illumina HiSeq2000 platform, PacBio platform and 10x genomics
330 platform, respectively. An inhouse quality control process was applied to the reads that
331 passed the Illumina quality filters. Firstly, adapters and primer sequences were
332 removed from the reads. Next, we discarded low-quality nucleotides (Q<30) from both
333 ends of the reads. Then, reads with N was more than 10% were removed. Finally, When
334 the number of low-quality (less than 5) bases in a single-end read exceeded 20%, the
335 pair end reads were discarded too. For Pacbio long reads datas, pre-assemble reads after
336 self-correction were used for genome assembly by Overlap-Layout-Consensus
337 algorithm in FALCON. Then, we used Illumina reads to perform sequence error
338 correction of contigs in Pilon(Walker et al., 2014). For 10 \times genomics data, the gel
339 beads are connected with: Illumine P5 connector, 16-base Barcodes, Illumina read 1
340 sequencing primer and 10 bp random sequence primers. The consensus sequences
341 were further scaffolded by integrating with 10 \times genomics linked reads by fragScaff
342 software(Adey et al., 2014). Others pipelines were according to standard processes of
343 Matware company’s standard process. Finally, all linked-reads were assist to Pacbio
344 datas for genome assembly.

345 **Hi-C sequencing and analysis.**

346 The harvestable young leaves of Seaside2000 were fixed with formaldehyde for
347 Hi-C sequencing. Approximately 3 g of leaf sample was collected and used for a Hi-C
348 pipeline as described in the publication(Xie et al., 2015). The Hi-C experiments were
349 performed by Matware company. The Hi-C libraries were then sequenced on an
350 Illumina HiSeq PE150 platform. Hi-C reads were aligned to the raw reference genome

351 SealIsle2000 for high assembly quality using BWA(Li and Durbin, 2009) and
352 LACHESIS with the default parameter settings(Burton et al., 2013).

353 **Assessment of genome assembly and annotation**

354 **Assessment of genome quality.**

355 The 1614 conserved protein models in the BUSCO niport yte_odb10 dataset
356 and the 242 conserved protein models in the CEGMA dataset were searched against the
357 SealIsle2000 genome by using the BUSCO (v5.2.2)(Manni et al., 2021) and the
358 CEGMA (v. 2.5)(Parra et al., 2007) programs with default parameters.

359 **Transposable element (TE) annotation.**

360 Chosen repeat libraries (RepBase; <http://www.girinst.org/repbase/>; Repeatmasker
361 and repeatproteinmask; <http://www.repeatmasker.org/>) and *de novo* prediction were
362 applied to identify repetitive elements. TE libraries were constructed with
363 RepeatModeler (<http://www.repeatmasker.org/>) and were applied to mask the
364 SealIsle2000 genomes by using RepeatMasker software with default parameters
365 (<http://www.repeatmasker.org/>).

366 **ncRNA_annotation.**

367 tRNAscan-SE (<http://lowelab.ucsc.edu/tRNAscan-SE/>) was used to identified
368 tRNA in the SealIsle2000 genome sequence. Since rRNA is highly conserved, rRNA
369 information of SealIsle2000 could be gained by blasting rRNA sequences of closely
370 related species to the reference genome. The miRNA and snRNA were predicted by
371 INFERNAL (<http://infernal.janelia.org/>).

372 **Gene prediction and function annotation.**

373 We performed an integrated approach combining PASA(Haas et al., 2003) and
374 EVM(Haas et al., 2008) pipelines. The predicted gene models from EVM were then
375 updated by PASA assembly alignments. Gene functions were assigned according to the

376 best alignment using BLASTP(Altschul et al., 1997) (Evalue <10⁻⁴) to the SwissProt
377 database (<http://www.uniprot.org/>) , Nr database
378 (<http://www.ncbi.nlm.nih.gov/protein>), Pfam database (<http://pfam.xfam.org/>), and the
379 KEGG database (<http://www.genome.jp/kegg>). The GO term for each gene was
380 achieved from the corresponding InterProScan.

381 Comparative Genomic and Evolutionary Analysis

382 Gene family Cluster and phylogenomic tree analysis.

383 To identify gene family, we analyzed protein-coding genes from 10 species,
384 *Sorghum bicolor* (*S. bicolor*), *Oryza sativa* (*O. sativa*), *Zea mays* (*Z. mays*), *Hordeum*
385 *vulgare* (*H. vulgare*), *Aegilops tauschii* (*A. tauschii*), *Setaria italica* (*S. italica*),
386 *Brachypodium distachyon* (*B. distachyon*), *Medicago truncatula* (*M. truncatula*),
387 *Arabidopsis thaliana* (*A. thaliana*), *Paspalum vaginatum* (*P. vaginatum*). Orthologous
388 gene groups of *P. vaginatum* and 9 other species were identified by the OrthoMCL
389 program(Li et al., 2003). Firstly, those genes with coding protein shorter than 50 amino
390 acids were filtered, and the longest transcript of one gene was kept when it contained
391 more than one transcript. Then, similarity between protein sequences of all species
392 were gained by blastp (e-value was less than 1e-5, both query and hit were more than
393 70% length coverage).

394 To infer the phylogenetic placements of *P. vaginatum*, single-copy genes of 10
395 species were extracted to align using MUSCLE (Edgar, 2004). The aligned results were
396 used to infer the maximum likelihood trees with RaxML(Stamatakis, 2006) . We used
397 the mcmcTree program of PAML (Yang, 2007) to estimate the divergence time among
398 10 species with main parameters (burn-in = 10,000, sample-number = 100,000, and
399 sample-frequency = 2). The calibration points were selected from TimeTree website
400 (<http://www.timetree.org>) as normal priors to restrain the age of the nodes,

401 Based on the phylogenetic tree and calibration points selected from TimeTree
402 website, we used the ‘mcmcTree’ module of PAML
403 (<http://abacus.gene.ucl.ac.uk/software/paml.html>) to estimate the divergence time of
404 these species.

405 **Analysis of genome synteny.**

406 The longest protein sequence of all genes was used to perform synteny searches to
407 identify syntenic genes of *S. paspalum* versus *S. bicolor* and *S. paspalum* versus *Z. mays* by using BLAST(Altschul et al., 1997) and MCScanX(Wang et al., 2012). Blastp
408 was used to search for potential anchors (E-value < 1e-10; top ten matches) between
409 each possible pair of chromosomes in multiple genomes. Then we used the
410 ‘circle_plotter’ and ‘bar_plotter’ of the downstream analyses programs to show the
411 syntenic genes.

413 **Population Analysis**

414 **Population Genome Resequencing and Detection of Nucleotide Variants.**

415 All clean reads from each accession were mapped to the Sealsle2000 reference
416 genome using BWA (Burrows-Wheeler Aligner)(Li and Durbin, 2009) (version 0.7.17)
417 using the mem function. Mapped reads were converted into BAM files using
418 SAMtools(Li et al., 2009), after removing duplicate reads, SNPs and InDels within the
419 193 accessions variants were called by Genome Analysis Toolkit (GATK) (version
420 3.4-46)(McKenna et al., 2010), the raw variants were filtered using the GATK
421 VariantFiltration tool with parameters as QD < 2.0 , MQ < 30.0 , FS > 60.0 ,SOR > 3.0,
422 MQRankSum < -12.5 , ReadPosRankSum < -8.0. Then to exclude SNP calling errors
423 caused by incorrect mapping or InDels, a total of 3,166,505 high-quality SNPs with
424 parameters as –max-missing 0.8 –maf 0.05 –mac 3 –minQ 30 –minDP 3 –min-alleles 2
425 –max-alleles 2, were kept for subsequent analysis. The identified InDels were filtered

426 using GATK filters (QD < 2.0 || FS > 200.0 || SOR > 10.0 || MQRankSum < -12.5 ||
427 ReadPosRankSum < -8.0). SNPs/ InDels annotation was performed on the basis of the
428 SeaIsle2000 genome with ANNOVAR (Wang et al., 2010) , SNPs/ InDels were
429 grouped into exon, intron, 5'-untranslated region and 3'-untranslated region, upstream
430 and downstream regions (within 1 kb region from the transcription start or stop site),
431 and intergenic regions. The SNPs/InDels in coding exons were further grouped into
432 synonymous or nonsynonymous mutations. The SNPs causing gain of a stop codon,
433 loss of a stop codon, or splicing were designated as large-effect SNPs. We further
434 classified InDels in coding exons as frameshift deletions or non-frameshift deletions
435 and the distribution of SNPs/InDels in the genome was demonstrated by
436 Circos(Krzywinski et al., 2009).

437 **Population structure and phylogenetic analyses.**

438 The population genetic structure was examined using the program sNMF (v1.2)
439 with K values from 2 to 10. We constructed a neighbor-joining tree with 3.08 million
440 SNPs using PHYLIP software and then visualized it with the online tool iTOL
441 (<https://itol.embl.de>). PCAs were done by GCTA(Yang et al., 2011). Nucleotide
442 diversity (π) and fixation index (FST) were calculated by Vcftools(Danecek et al., 2011)
443 with a 200kb sliding window. To estimate and compare the pattern of LD among
444 different groups, the squared correlation coefficient (r^2) between pairwise SNPs was
445 computed and plotted using the PopLDdecay (v.3.40)(Zhang et al., 2019) software.
446 Parameters in the program were MaxDist 500. The average r^2 value was calculated for
447 pairwise markers in a 500-kb window and averaged across the whole genome.

448 **Phenotypic data for salt tolerance**

449 After treatment with salt solution, the symptoms of salt damage in the leaves were
450 assessed visually. Seventy-six germplasms of *P. vaginatum* were chosen from the lawn

451 grass germplasm garden, all materials were propagated from healthy stolons gathered
452 from their native habitat and planted in the experimental field of Danzhou campus of
453 Hainan University. From July 15 to November 25 in 2019, each variety was
454 acclimatized from the same number of tillers, planted in four 5.5×5.5 cm circular
455 containers and place on gauze-based foam board (30 cm×30 cm), with hydroponic
456 culture conditions using Hoagland's nutrient medium in a greenhouse with an average
457 temperature from 28 °C to 36 °C. The Hoagland's nutrient solution was replaced once
458 every week for about ten weeks until each circular container was covered with grass
459 and had the same growth state. The experimental design was a randomized block
460 design with 2 treatments (control and salt treatment), and 3 replications for each
461 treatment. At first, salt treatment was performed with 32 ds·m⁻¹ NaCl for 3 days, the
462 visual reactions of plant under salt stress were evaluated using wilting degree (WD3)
463 and withering rates (WR3). Then NaCl was added to 54 ds·m⁻¹ until the 7th day, wilting
464 degree (WD7) and withering rates (WR7) were measured again.

465 **FST and ROD analysis and selective sweep detection**

466 The top 20 salt-tolerant germplasms were named ST while the most 20
467 sensitive-salt germplasms were named ST according to their phenotype after salt
468 stress. Nucleotide diversity (π), fixation index (FST) and reduction of diversity ROD
469 were calculated by Vcftools(Danecek et al., 2011) with a 200 kb sliding window with a
470 step size of 20 kb. ggplot2(Wickham, 2016) in the R packages was applied for
471 presentation.

472 **Genome-wide association study**

473 Only SNPs with MAF \geq 0.05 and missing rate \leq 0.2 in a population were used to
474 carry out GWAS. This resulted in 2,221,123 SNPs that were used in GWAS for 76 *P.*
475 *vaginatum* germplasms. We performed GWAS using EMMAX software. Significant

476 *P*-value (0.05/n, Bonferroni correction) and suggestive *P*-value (10^{-6}) were set to
477 control the genome-wide type I error rate. The results of GEMMA were visualized as
478 Manhattan and Q-Q plots with the R package ‘Cmplot’. We then selected genes near
479 the peak SNPs according to the Manhattan plot for each trait and annotated candidate
480 genes.

481

482 **GO terms and KEGG pathway enrichment analysis**

483 Based on the annotation information
484 (<http://eggnog-mapper.embl.de/>)(Huerta-Cepas et al., 2017), candidate genes were
485 analyzed by GO terms and KEGG pathway functional enrichment using clusterProfiler
486 under the R platform (v4.0.2). GO terms and KEGG pathways with Q-values < 0.05
487 were considered to be significantly enriched.

488 **Transcriptome analysis and genetic authentication**

489 Total RNA was isolated from a sampled organ with three biological replicates at
490 different stress stages to investigate expression of the genes associated with salt
491 tolerance for roots and leaves. RNA extraction and library preparation for each sample
492 were performed by Matware company. All 64 samples with three biological replicates
493 were sequenced using the Illumina HiSeq 2000 platform, and 150 bp pairedend reads
494 were generated. After filtering, 2,464,855,778 clean reads were obtained, containing
495 369.73 Gb of data. On average, 88.37% of the reads uniquely mapped to the
496 Sealsle2000 reference genome ([Table S23](#)). Analysis of differential gene expression
497 between two samples was performed using the DESeq R package (v1.18.0). Genes with
498 an adjusted P value < 0.05 found by DESeq were assigned as differentially expressed.

499 *A. thaliana* was used for transformation in the present study. To generate
500 *PvHKT7* overexpression lines, a 1806-bp coding sequence (CDS) of *PvHKT7* was

501 amplified from cDNA of Sea Isle 2000 and verified by sequencing, using the primer set
502 listed in Supplementary Table S27. The gene entry vector and expression vector were
503 constructed by enzyme digestion ligand and Plasmid DNA was extracted using a
504 plasmid microextraction kit (MEgi bio). Transgenic *A. thaliana* seeds of T2
505 generation and WT generation were cultured on LB medium plate (32 ds·m⁻¹ NaCl
506 and normal) at 25 °C for 10 days

507 **Contributions**

508 Li Liao, Xu Hu, Jiangshan Hao and Minqiang Tang contributed equally to this work.
509 Jie Luo and Zhiyong Wang conceived and managed the project. Li Liao, Shangqian
510 Xie and Minqiang Tang designed the experiments. Longzhou Ren performed
511 molecular cloning and salt stress experiments. Xu Hu and Jiangshan Hao performed
512 data analyses and wrote the manuscript. Ling Pan, Paul Raymer, Peng Qi and
513 Zhenbang Chen interpreted the results and revised the manuscript.

514

515 **Data available**

516 The raw sequence data of *P. vaginatum* genome project has been deposited at the The
517 National Center for Biotechnology Information under BioProject PRJNA848273. The
518 final assembly and gene annotation of *P. vaginatum* is available at GenBank under the
519 accession number SUB11601520.

520

521 **Acknowledgements**

522 We sincerely acknowledge the Katrien M. Devos, which is a professor of University
523 of Georgia, for a critical reading of the manuscript and valuable discussions. This
524 work was supported by the National Natural Science Foundation of China
525 (No.32060409), the Construction of World First Class Discipline of Hainan
526 University (No.RZZX201905) and National Project on Sci-Tec Foundation Resources
527 Survey (2017FY100600).

528

529 **References**

530 **Acosta-Motos JR, Ortuno MF, Bernal-Vicente A, Diaz-Vivancos P,**

531 **Sanchez-Blanco MJ, Hernandez JA** (2017) Plant Responses to Salt Stress
 532 Adaptive Mechanisms. *Agronomy-Basel* 7

533 **Adey A, Kitzman JO, Burton JN, Daza R, Kumar A, Christiansen L, Ronaghi M, Amini S, Gunderson KL, Steemers FJ, Shendure J** (2014) In vitro, 534 long-range sequence information for de novo genome assembly via transposase 535 contiguity. *Genome Research* 24: 2041-2049

536 **Altschul SF, Madden TL, Schaffer AA, Zhang J, Zhang Z, Miller W, Lipman DJ** 537 (1997) Gapped BLAST and PSI-BLAST: a new generation of protein database 538 search programs. *Nucleic Acids Res* 25: 3389-3402

539 **Burton JN, Adey A, Patwardhan RP, Qiu R, Kitzman JO, Shendure J** (2013) 540 Chromosome-scale scaffolding of de novo genome assemblies based on 541 chromatin interactions. *Nat Biotechnol* 31: 1119-1125

542 **Calone R, Sanoubar R, Lambertini C, Speranza M, Antisari LV, Vianello G, Barbanti L** (2020) Salt Tolerance and Na Allocation in Sorghum bicolor under 543 Variable Soil and Water Salinity. *Plants (Basel)* 9

544 **Catching KE, LaFayette PR, Parrott WA, Raymer PL** (2019) Engineering Dollar 545 Spot Resistance in *Paspalum vaginatum* (Seashore Paspalum) by Bioloistic Gene 546 Transformation. In *Vitro Cellular & Developmental Biology-Animal* 55: 547 S71-S72

548 **Chen ZB, Kim W, Newman M, Wang ML, Raymer P** (2005) Molecular 549 characterization of genetic diversity in the USDA seashore *paspalum* 550 germplasm collection. *International Turfgrass Society Research Journal* 10: 551 543-549

552 **Danecek P, Auton A, Abecasis G, Albers CA, Banks E, DePristo MA, Handsaker 553 RE, Lunter G, Marth GT, Sherry ST, McVean G, Durbin R, Genomes Project 554 Analysis G** (2011) The variant call format and VCFtools. *Bioinformatics* 27: 2156-2158

555 **Edgar RC** (2004) MUSCLE: multiple sequence alignment with high accuracy and 556 high throughput. *Nucleic Acids Res* 32: 1792-1797

557 **Eudy D, Bahri BA, Harrison ML, Raymer P, Devos KM** (2017) Ploidy Level and 558 Genetic Diversity in the Genus *Paspalum*, Group *Disticha*. *Crop Science* 57: 559 3319-3332

560 **Farooq M, Hussain M, Wakeel A, Siddique KHM** (2015) Salt stress in maize: 561 effects, resistance mechanisms, and management. A review. *Agronomy for 562 Sustainable Development* 35: 461-481

563 **Haas BJ, Delcher AL, Mount SM, Wortman JR, Smith Jr RK, Hannick LI, Maiti 564 R, Ronning CM, Rusch DB, Town CD** (2003) Improving the *Arabidopsis* 565 genome annotation using maximal transcript alignment assemblies. *Nucleic 566 acids research* 31: 5654-5666

567 **Haas BJ, Salzberg SL, Zhu W, Pertea M, Allen JE, Orvis J, White O, Buell CR, 568 Wortman JR** (2008) Automated eukaryotic gene structure annotation using 569 EVidenceModeler and the Program to Assemble Spliced Alignments. *Genome 570 Biol* 9: R7

571 **Huerta-Cepas J, Forslund K, Coelho LP, Szklarczyk D, Jensen LJ, von Mering C, 572 Bork P** (2017) Fast Genome-Wide Functional Annotation through Orthology 573 Assignment by eggNOG-Mapper. *Molecular Biology and Evolution* 34: 574 2115-2122

575 **Kang HM, Sul JH, Service SK, Zaitlen NA, Kong SY, Freimer NB, Sabatti C, Eskin E** (2010) Variance component model to account for sample structure in 576 577

580 genome-wide association studies. *Nature Genetics* **42**: 348-U110
581 **Krzywinski M, Schein J, Birol I, Connors J, Gascoyne R, Horsman D, Jones SJ,**
582 **Marra MA** (2009) Circos: An information aesthetic for comparative genomics.
583 *Genome Research* **19**: 1639-1645
584 **Li H, Durbin R** (2009) Fast and accurate short read alignment with Burrows-Wheeler
585 transform. *Bioinformatics* **25**: 1754-1760
586 **Li H, Handsaker B, Wysoker A, Fennell T, Ruan J, Homer N, Marth G, Abecasis**
587 **G, Durbin R, Proc GPD** (2009) The Sequence Alignment/Map format and
588 SAMtools. *Bioinformatics* **25**: 2078-2079
589 **Li L, Stoeckert CJ, Jr., Roos DS** (2003) OrthoMCL: identification of ortholog groups
590 for eukaryotic genomes. *Genome Res* **13**: 2178-2189
591 **Liu Y, Liu J, Xu L, Lai H, Chen Y, Yang ZM, Huang BR** (2017) Identification and
592 Validation of Reference Genes for Seashore Paspalum Response to Abiotic
593 Stresses. *International Journal of Molecular Sciences* **18**
594 **Liu Z-W, Jarret RL, Duncan RR, Kresovich S** (1994) Genetic relationships and
595 variation among ecotypes of seashore paspalum (*Paspalum vaginatum*)
596 determined by random amplified polymorphic DNA markers. *Genome* **37**:
597 1011-1017
598 **Manni M, Berkeley MR, Seppey M, Simao FA, Zdobnov EM** (2021) BUSCO
599 Update: Novel and Streamlined Workflows along with Broader and Deeper
600 Phylogenetic Coverage for Scoring of Eukaryotic, Prokaryotic, and Viral
601 Genomes. *Mol Biol Evol* **38**: 4647-4654
602 **McKenna A, Hanna M, Banks E, Sivachenko A, Cibulskis K, Kernytsky A,**
603 **Garimella K, Altshuler D, Gabriel S, Daly M, DePristo MA** (2010) The
604 Genome Analysis Toolkit: a MapReduce framework for analyzing
605 next-generation DNA sequencing data. *Genome Res* **20**: 1297-1303
606 **Parra G, Bradnam K, Korf I** (2007) CEGMA: a pipeline to accurately annotate core
607 genes in eukaryotic genomes. *Bioinformatics* **23**: 1061-1067
608 **Qi P, Eudy D, Schnable JC, Schmutz J, Raymer PL, Devos KM** (2019) High
609 Density Genetic Maps of Seashore Paspalum Using
610 Genotyping-By-Sequencing and Their Relationship to The Sorghum Bicolor
611 Genome. *Scientific Reports* **9**
612 **Roy SJ, Negrao S, Tester M** (2014) Salt resistant crop plants. *Current Opinion in*
613 *Biotechnology* **26**: 115-124
614 **Shen Q, Bian H, Wei HY, Liao L, Wang ZY, Luo XY, Ding XP, Chen ZB, Raymer**
615 **P** (2020) Genetic Diversity of Seashore Paspalum Revealed with Simple
616 Sequence Repeat Markers. *Journal of the American Society for Horticultural*
617 *Science* **145**: 228-235
618 **Stamatakis A** (2006) RAxML-VI-HPC: maximum likelihood-based phylogenetic
619 analyses with thousands of taxa and mixed models. *Bioinformatics* **22**:
620 2688-2690
621 **Walker BJ, Abeel T, Shea T, Priest M, Abouelliel A, Sakthikumar S, Cuomo CA,**
622 **Zeng Q, Wortman J, Young SK, Earl AM** (2014) Pilon: an integrated tool for
623 comprehensive microbial variant detection and genome assembly
624 improvement. *PLoS One* **9**: e112963
625 **Wang K, Li MY, Hakonarson H** (2010) ANNOVAR: functional annotation of
626 genetic variants from high-throughput sequencing data. *Nucleic Acids*
627 *Research* **38**
628 **Wang YP, Tang HB, DeBarry JD, Tan X, Li JP, Wang XY, Lee TH, Jin HZ,**

629 **Marler B, Guo H, Kissinger JC, Paterson AH** (2012) MCScanX: a toolkit for
630 detection and evolutionary analysis of gene synteny and collinearity. *Nucleic
631 Acids Research* **40**

632 **Wickham H** (2016) *ggplot2 : Elegant Graphics for Data Analysis. In Use R!*, Ed 2nd.
633 Springer International Publishing : Imprint: Springer,, Cham, pp 1 online
634 resource (XVI, 260 pages 232 illustrations, 140 illustrations in color)

635 **Wu PP, Cogill S, Qiu YJ, Li ZG, Zhou M, Hu Q, Chang ZH, Noorai RE, Xia XX, Sasaki C, Raymer P, Luo H** (2020) Comparative transcriptome profiling provides insights into plant salt tolerance in seashore paspalum (*Paspalum vaginatum*). *Bmc Genomics* **21**

636 **Wu XL, Shi HF, Guo ZF** (2018) Overexpression of a NF-YC Gene Results in Enhanced Drought and Salt Tolerance in Transgenic Seashore Paspalum. *Frontiers in Plant Science* **9**

637 **Xie T, Zheng JF, Liu S, Peng C, Zhou YM, Yang QY, Zhang HY** (2015) De Novo Plant Genome Assembly Based on Chromatin Interactions: A Case Study of *Arabidopsis thaliana*. *Molecular Plant* **8**: 489-492

638 **Yang J, Lee SH, Goddard ME, Visscher PM** (2011) GCTA: a tool for genome-wide complex trait analysis. *Am J Hum Genet* **88**: 76-82

639 **Yang Z** (2007) PAML 4: phylogenetic analysis by maximum likelihood. *Mol Biol Evol* **24**: 1586-1591

640 **Zhang C, Dong SS, Xu JY, He WM, Yang TL** (2019) PopLDdecay: a fast and effective tool for linkage disequilibrium decay analysis based on variant call format files. *Bioinformatics* **35**: 1786-1788

641

642

643

644

645

646

647

648

649

650

651

652

653 **Supplementary Information**

654 Supplementary Fig.

655 Supplementary Table

656

657 Tables

658 **Table 1 Summary statistics of the *P. vaginatum* genome assembly**

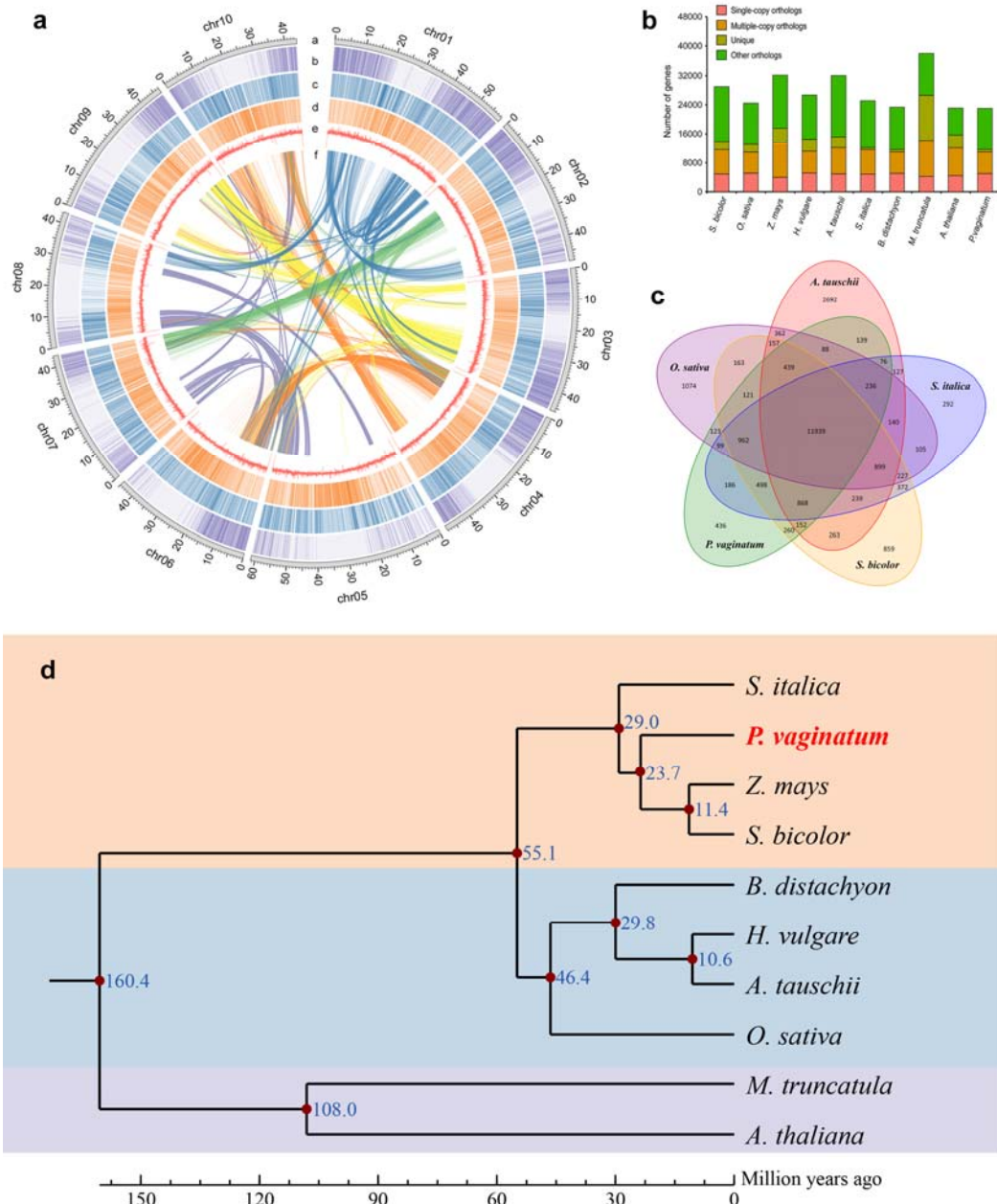
Category	Sea Isle2000
Assembly size (Mb)	517.98
Contig N50 (Mb)	5.12
Scaffold N50 (Mb)	47.06
Chromosome-scale scaffolds (Mb)	485.64 (93.76%)

Repeat content (%)	49.22
GC content (%)	45.85
Heterozygosity rate (%)	0.81
Number of protein-coding genes	28,712

659

660

661 Figures

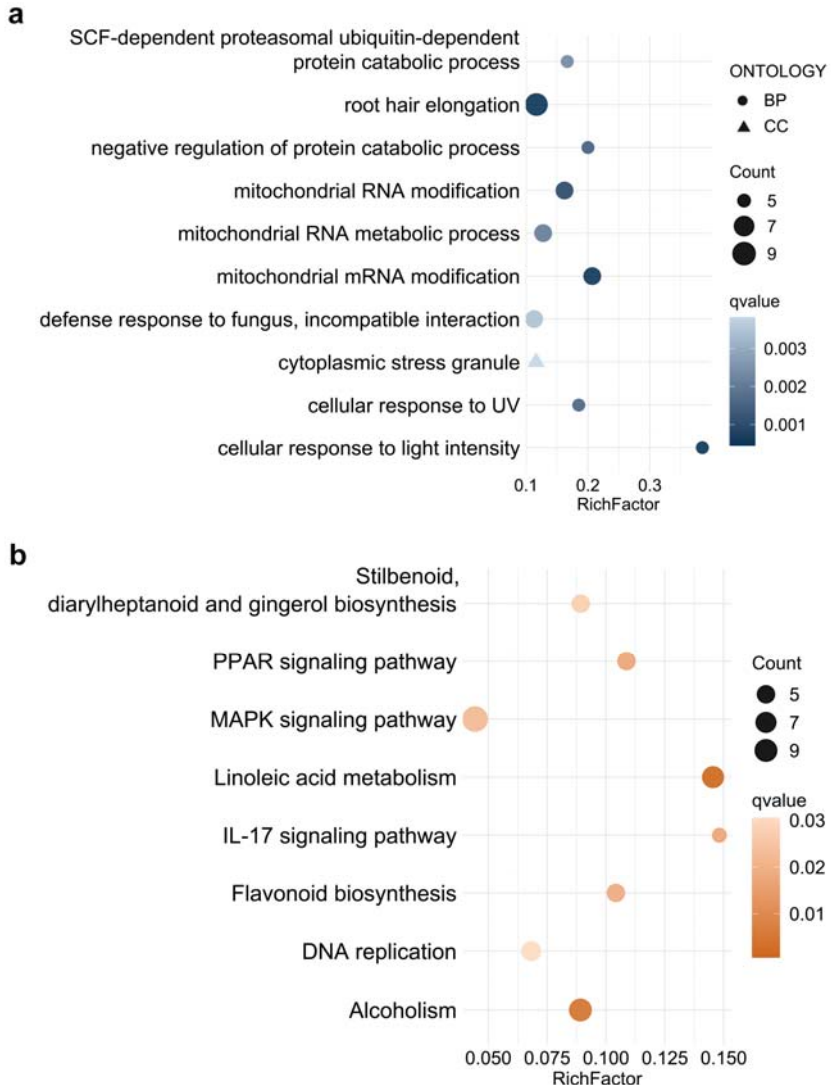


662

663 **Fig. 1 Genome evolutionary history.** **a** Chromosomal features and synteny landscape
664 of *P. vaginatum* genome. **a**, Chromosome size with units in Mb. **b**, Gene density. **c**,
665 Indel density. **d**, SNP density. **e**, GC content. **f**, Genome syntenic blocks are illustrated
666 with colored lines. **b** The distribution of single-copy, multiple-copy, unique, and other
667 orthologs in the 9 plant species. **c** Venn diagram represents the shared and unique gene
668 families among five species. Each number represents the number of gene families,
669 numbers in the non-overlapped circles represent the number of gene families were
670 specific to the species. **d** Phylogenetic tree of 10 plant species. Blue numbers represent
671 divergence time of each node. The divergence time between the monocots and eudicots
672 were estimated to be 138.2-190.0 million years ago (Ma).

673

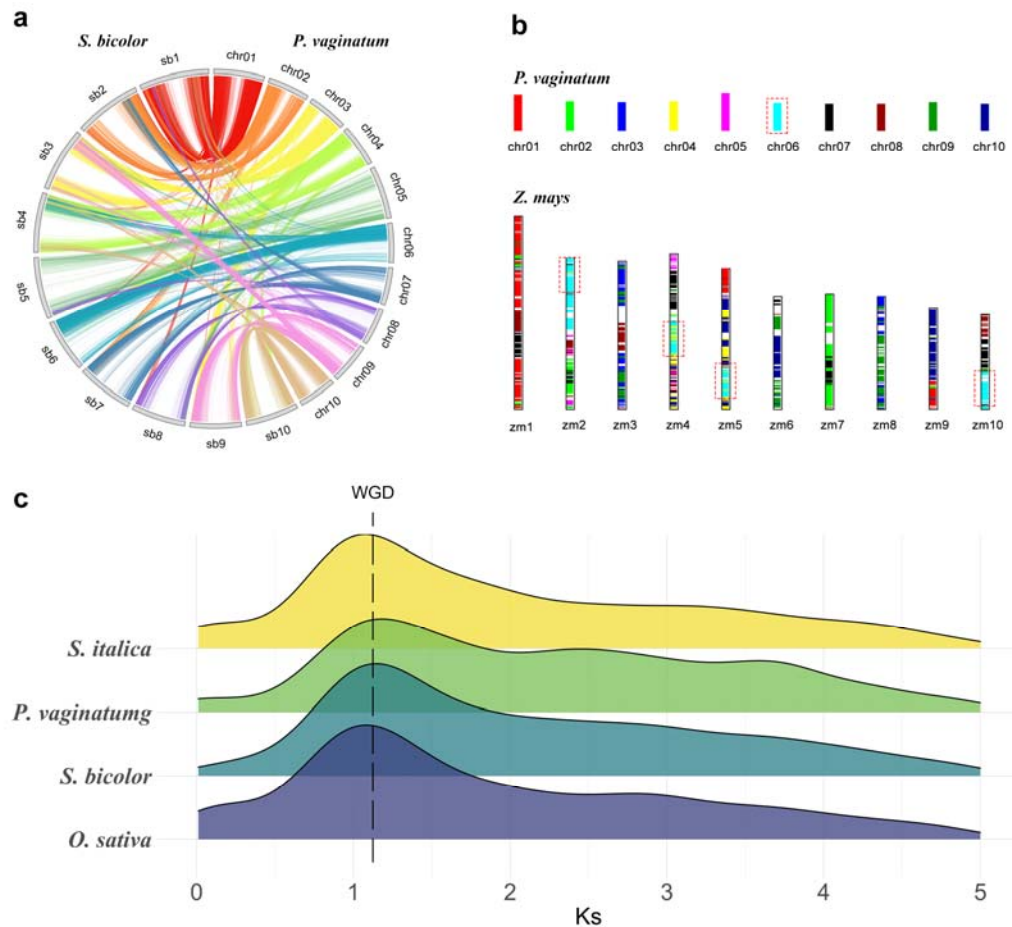
674



675

676 **Fig. 2 Enrichment analysis of specific genes in *P. vaginatum*.** **a** The enriched GO
677 terms with top 15 RichFactor were presented. The color of circles represents the
678 statistical significance of enriched GO terms. The size of the circles represents the
679 number of genes in a GO term. **b** The enriched KEGG pathways with corrected qvalue
680 < 0.05 were presented. The color of circles represents the statistical significance of
681 enriched KEGG pathways. The size of the circles represents the number of genes in a
682 KEGG pathway.

683

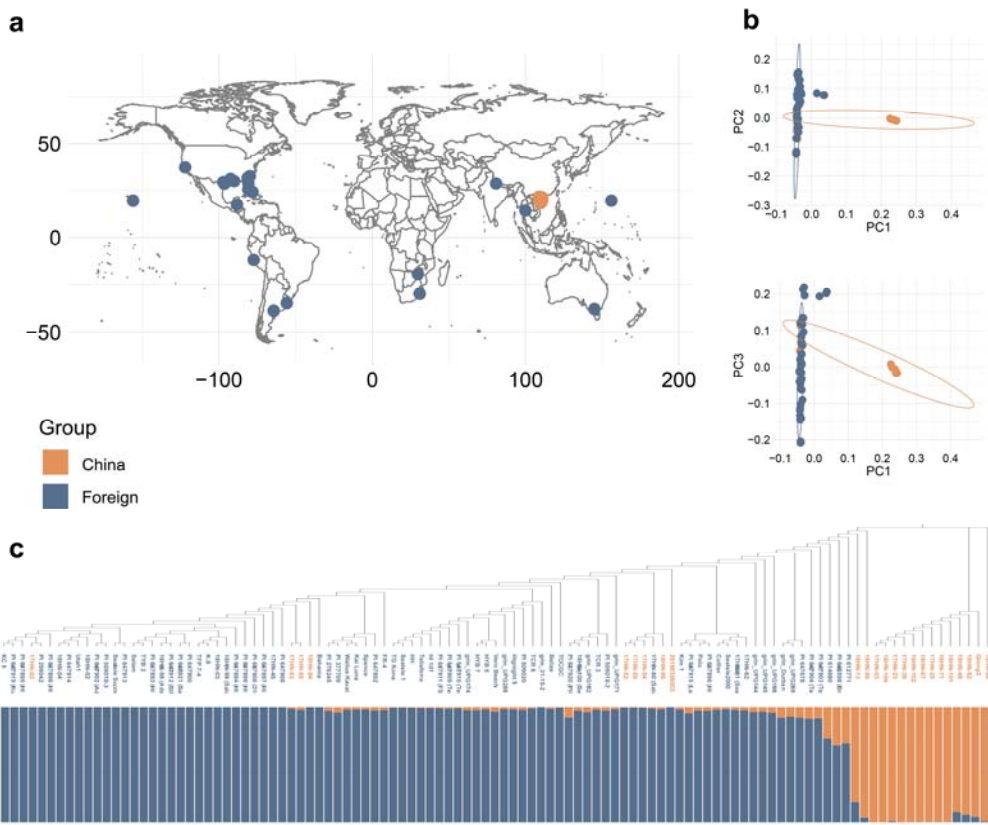


684
685 **Fig. 3** syntenic genes of *P. vaginatum*, *S. bicolor*, *Z. mays*. **a** the relationship of
686 syntenic genes of *P. vaginatum* and *S. bicolor*. **b** the relationship of syntenic genes of *P.*
687 *vaginatum* and *Z. mays*. Different colors mean different chromosomes in *P. vaginatum*
688 genome, the corresponding color in *Z. mays* chromosomes mean that genes are syntenic
689 with those genes located on corresponding chromosomes in *P. vaginatum* genome. Red
690 dotted boxes show a case of the genes in chromosome 6 of *P. vaginatum* that have four
691 copies in *Z. mays*. **c** Distribution of synonymous substitution rates (Ks) among collinear
692 paralogs in four plants.

693

694

695



696

697 **Fig. 4. Geographical distribution and population structure of *P. vaginatum***
698 **accessions. a** Geographic distributions of 107 *P. vaginatum* accessions. **b** PCA plots
699 showing two divergent clades of 107 *P. vaginatum* accessions. **c** The NJ phylogeny of
700 107 *P. vaginatum* accessions and model-based clustering with K = 2.

701

702

703

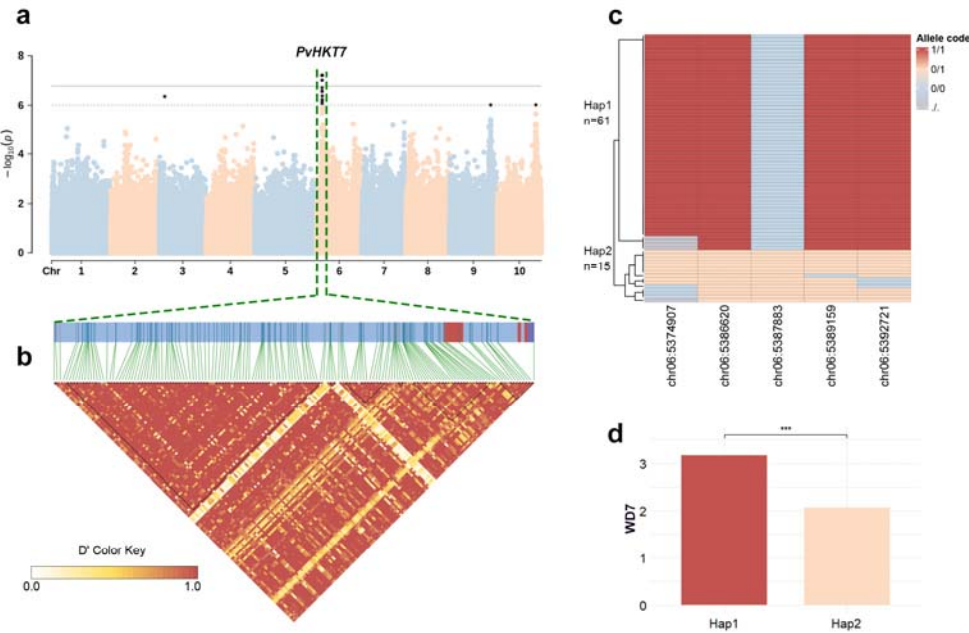
704

705

706

707

708



709

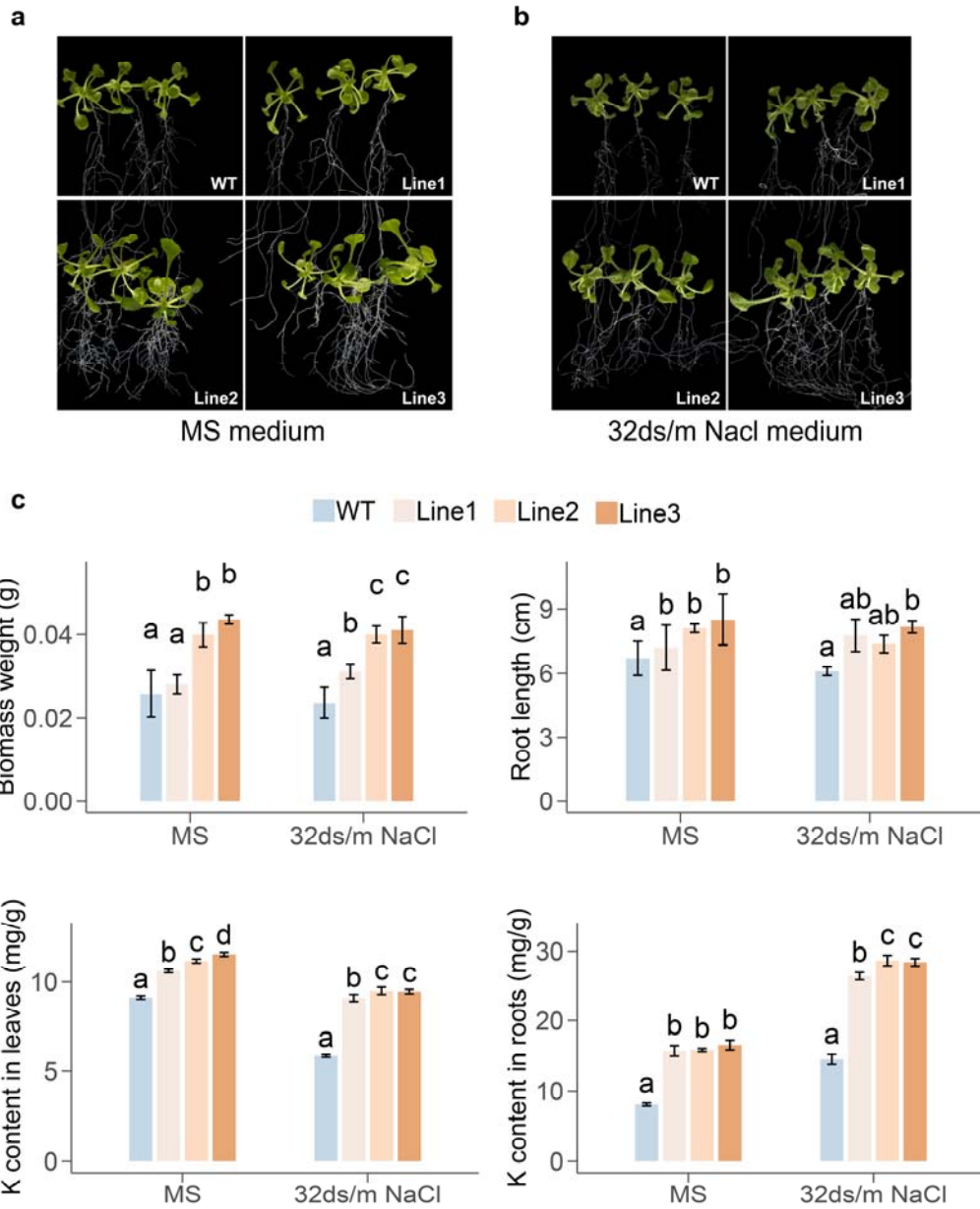
710 **Fig. 5 Genome-wide identification of candidate genes associated with salt**
711 **tolerance. a** Manhattan plot of the salt tolerance trait on the chromosome 6. **b** LD heat
712 map of the *PvHKT7* gene. The color key indicates D' values. **c** Haplotypes for the
713 candidate gene *PvHKT7*. **d** The SNP genotype is associated with the salt tolerance
714 phenotype.

715

716

717

718



719
720 **Fig. 6 Transgenic verification.** **a** The growth of non-transgenic (WT) and transgenic
721 (Line1, Line2, Line3) *A. thaliana* exposed to 1/2 MS medium. **b** The growth of
722 non-transgenic (WT) and transgenic (Line1, Line2, Line3) *A. thaliana* exposed to 32
723 ds·m⁻¹ NaCl MS medium. **c** Difference analysis of biomass weight and root length
724 between A and B non-transgenic and transgenic *A. thaliana*.

725
726

Parsed Citations

Acosta-Motos JR, Ortuno MF, Bernal-Vicente A, Diaz-Vivancos P, Sanchez-Blanco MJ, Hernandez JA (2017) Plant Responses to Salt Stress: Adaptive Mechanisms. *Agronomy-Basel* 7
Google Scholar: [Author Only](#) [Title Only](#) [Author and Title](#)

Adey A, Kitzman JO, Burton JN, Daza R, Kumar A, Christiansen L, Ronaghi M, Amini S, Gunderson KL, Steemers FJ, Shendure J (2014) In vitro, long-range sequence information for de novo genome assembly via transposase contiguity. *Genome Research* 24: 2041-2049
Google Scholar: [Author Only](#) [Title Only](#) [Author and Title](#)

Altschul SF, Madden TL, Schaffer AA, Zhang J, Zhang Z, Miller W, Lipman DJ (1997) Gapped BLAST and PSI-BLAST: a new generation of protein database search programs. *Nucleic Acids Res* 25: 3389-3402
Google Scholar: [Author Only](#) [Title Only](#) [Author and Title](#)

Burton JN, Adey A, Patwardhan RP, Qiu R, Kitzman JO, Shendure J (2013) Chromosome-scale scaffolding of de novo genome assemblies based on chromatin interactions. *Nat Biotechnol* 31: 1119-1125
Google Scholar: [Author Only](#) [Title Only](#) [Author and Title](#)

Calone R, Sanoubar R, Lambertini C, Speranza M, Antisari LV, Vianello G, Barbanti L (2020) Salt Tolerance and Na Allocation in Sorghum bicolor under Variable Soil and Water Salinity. *Plants (Basel)* 9
Google Scholar: [Author Only](#) [Title Only](#) [Author and Title](#)

Catching KE, LaFayette PR, Parrott WA, Raymer PL (2019) Engineering Dollar Spot Resistance in *Paspalum vaginatum* (Seashore Paspalum) by Biolistic Gene Transformation. *In Vitro Cellular & Developmental Biology-Animal* 55: S71-S72
Google Scholar: [Author Only](#) [Title Only](#) [Author and Title](#)

Chen ZB, Kim W, Newman M, Wang ML, Raymer P (2005) Molecular characterization of genetic diversity in the USDA seashore paspalum germplasm collection. *International Turfgrass Society Research Journal* 10: 543-549
Google Scholar: [Author Only](#) [Title Only](#) [Author and Title](#)

Danecek P, Auton A, Abecasis G, Albers CA, Banks E, DePristo MA, Handsaker RE, Lunter G, Marth GT, Sherry ST, McVean G, Durbin R, Genomes Project Analysis G (2011) The variant call format and VCFtools. *Bioinformatics* 27: 2156-2158
Google Scholar: [Author Only](#) [Title Only](#) [Author and Title](#)

Edgar RC (2004) MUSCLE: multiple sequence alignment with high accuracy and high throughput. *Nucleic Acids Res* 32: 1792-1797
Google Scholar: [Author Only](#) [Title Only](#) [Author and Title](#)

Eudy D, Bahri BA, Harrison ML, Raymer P, Devos KM (2017) Ploidy Level and Genetic Diversity in the Genus *Paspalum*, Group Disticha. *Crop Science* 57: 3319-3332
Google Scholar: [Author Only](#) [Title Only](#) [Author and Title](#)

Farooq M, Hussain M, Wakeel A, Siddique KHM (2015) Salt stress in maize: effects, resistance mechanisms, and management. A review. *Agronomy for Sustainable Development* 35: 461-481
Google Scholar: [Author Only](#) [Title Only](#) [Author and Title](#)

Haas BJ, Delcher AL, Mount SM, Wortman JR, Smith Jr RK, Hannick LI, Maiti R, Ronning CM, Rusch DB, Town CD (2003) Improving the *Arabidopsis* genome annotation using maximal transcript alignment assemblies. *Nucleic acids research* 31: 5654-5666
Google Scholar: [Author Only](#) [Title Only](#) [Author and Title](#)

Haas BJ, Salzberg SL, Zhu W, Pertea M, Allen JE, Orvis J, White O, Buell CR, Wortman JR (2008) Automated eukaryotic gene structure annotation using EvidenceModeler and the Program to Assemble Spliced Alignments. *Genome Biol* 9: R7
Google Scholar: [Author Only](#) [Title Only](#) [Author and Title](#)

Huerta-Cepas J, Forslund K, Coelho LP, Szklarczyk D, Jensen LJ, von Mering C, Bork P (2017) Fast Genome-Wide Functional Annotation through Orthology Assignment by eggNOG-Mapper. *Molecular Biology and Evolution* 34: 2115-2122
Google Scholar: [Author Only](#) [Title Only](#) [Author and Title](#)

Kang HM, Sul JH, Service SK, Zaitlen NA, Kong SY, Freimer NB, Sabatti C, Eskin E (2010) Variance component model to account for sample structure in genome-wide association studies. *Nature Genetics* 42: 348-U110
Google Scholar: [Author Only](#) [Title Only](#) [Author and Title](#)

Krzywinski M, Schein J, Birol I, Connors J, Gascoyne R, Horsman D, Jones SJ, Marra MA (2009) Circos: An information aesthetic for comparative genomics. *Genome Research* 19: 1639-1645
Google Scholar: [Author Only](#) [Title Only](#) [Author and Title](#)

Li H, Durbin R (2009) Fast and accurate short read alignment with Burrows-Wheeler transform. *Bioinformatics* 25: 1754-1760
Google Scholar: [Author Only](#) [Title Only](#) [Author and Title](#)

Li H, Handsaker B, Wysoker A, Fennell T, Ruan J, Homer N, Marth G, Abecasis G, Durbin R, Proc GPD (2009) The Sequence Alignment/Map format and SAMtools. Bioinformatics 25: 2078-2079

Google Scholar: [Author Only](#) [Title Only](#) [Author and Title](#)

Li L, Stoeckert CJ, Jr., Roos DS (2003) OrthoMCL: identification of ortholog groups for eukaryotic genomes. Genome Res 13: 2178-2189

Google Scholar: [Author Only](#) [Title Only](#) [Author and Title](#)

Liu Y, Liu J, Xu L, Lai H, Chen Y, Yang ZM, Huang BR (2017) Identification and Validation of Reference Genes for Seashore Paspalum Response to Abiotic Stresses. International Journal of Molecular Sciences 18

Google Scholar: [Author Only](#) [Title Only](#) [Author and Title](#)

Liu Z-W, Jarret RL, Duncan RR, Kresovich S (1994) Genetic relationships and variation among ecotypes of seashore paspalum (*Paspalum vaginatum*) determined by random amplified polymorphic DNA markers. Genome 37: 1011-1017

Google Scholar: [Author Only](#) [Title Only](#) [Author and Title](#)

Manni M, Berkeley MR, Seppey M, Simao FA, Zdobnov EM (2021) BUSCO Update: Novel and Streamlined Workflows along with Broader and Deeper Phylogenetic Coverage for Scoring of Eukaryotic, Prokaryotic, and Viral Genomes. Mol Biol Evol 38: 4647-4654

Google Scholar: [Author Only](#) [Title Only](#) [Author and Title](#)

McKenna A, Hanna M, Banks E, Sivachenko A, Cibulskis K, Kernytsky A, Garimella K, Altshuler D, Gabriel S, Daly M, DePristo MA (2010) The Genome Analysis Toolkit: a MapReduce framework for analyzing next-generation DNA sequencing data. Genome Res 20: 1297-1303

Google Scholar: [Author Only](#) [Title Only](#) [Author and Title](#)

Parra G, Bradnam K, Korf I (2007) CEGMA: a pipeline to accurately annotate core genes in eukaryotic genomes. Bioinformatics 23: 1061-1067

Google Scholar: [Author Only](#) [Title Only](#) [Author and Title](#)

Qi P, Eudy D, Schnable JC, Schmutz J, Raymer PL, Devos KM (2019) High Density Genetic Maps of Seashore Paspalum Using Genotyping-By-Sequencing and Their Relationship to The Sorghum Bicolor Genome. Scientific Reports 9

Google Scholar: [Author Only](#) [Title Only](#) [Author and Title](#)

Roy SJ, Negrao S, Tester M (2014) Salt resistant crop plants. Current Opinion in Biotechnology 26: 115-124

Google Scholar: [Author Only](#) [Title Only](#) [Author and Title](#)

Shen Q, Bian H, Wei HY, Liao L, Wang ZY, Luo XY, Ding XP, Chen ZB, Raymer P (2020) Genetic Diversity of Seashore Paspalum Revealed with Simple Sequence Repeat Markers. Journal of the American Society for Horticultural Science 145: 228-235

Google Scholar: [Author Only](#) [Title Only](#) [Author and Title](#)

Stamatakis A (2006) RAxML-VI-HPC: maximum likelihood-based phylogenetic analyses with thousands of taxa and mixed models. Bioinformatics 22: 2688-2690

Google Scholar: [Author Only](#) [Title Only](#) [Author and Title](#)

Walker BJ, Abeel T, Shea T, Priest M, Abouelliel A, Sakthikumar S, Cuomo CA, Zeng Q, Wortman J, Young SK, Earl AM (2014) Pilon: an integrated tool for comprehensive microbial variant detection and genome assembly improvement. PLoS One 9: e112963

Google Scholar: [Author Only](#) [Title Only](#) [Author and Title](#)

Wang K, Li MY, Hakonarson H (2010) ANNOVAR: functional annotation of genetic variants from high-throughput sequencing data. Nucleic Acids Research 38

Google Scholar: [Author Only](#) [Title Only](#) [Author and Title](#)

Wang YP, Tang HB, DeBarry JD, Tan X, Li JP, Wang XY, Lee TH, Jin HZ, Marler B, Guo H, Kissinger JC, Paterson AH (2012) MCScanX: a toolkit for detection and evolutionary analysis of gene synteny and collinearity. Nucleic Acids Research 40

Google Scholar: [Author Only](#) [Title Only](#) [Author and Title](#)

Wickham H (2016) ggplot2 : Elegant Graphics for Data Analysis. In Use R!, Ed 2nd. Springer International Publishing : Imprint: Springer,, Cham, pp 1 online resource (XV, 260 pages 232 illustrations, 140 illustrations in color

Google Scholar: [Author Only](#) [Title Only](#) [Author and Title](#)

Wu PP, Cogill S, Qiu YJ, Li ZG, Zhou M, Hu Q, Chang ZH, Noorai RE, Xia XX, Saski C, Raymer P, Luo H (2020) Comparative transcriptome profiling provides insights into plant salt tolerance in seashore paspalum (*Paspalum vaginatum*). Bmc Genomics 21

Google Scholar: [Author Only](#) [Title Only](#) [Author and Title](#)

Wu XL, Shi HF, Guo ZF (2018) Overexpression of a NF-YC Gene Results in Enhanced Drought and Salt Tolerance in Transgenic Seashore Paspalum. Frontiers in Plant Science 9

Google Scholar: [Author Only](#) [Title Only](#) [Author and Title](#)

Xie T, Zheng JF, Liu S, Peng C, Zhou YM, Yang QY, Zhang HY (2015) De Novo Plant Genome Assembly Based on Chromatin Interactions: A Case Study of *Arabidopsis thaliana*. *Molecular Plant* 8: 489-492

Google Scholar: [Author Only](#) [Title Only](#) [Author and Title](#)

Yang J, Lee SH, Goddard ME, Visscher PM (2011) GCTA: a tool for genome-wide complex trait analysis. *Am J Hum Genet* 88: 76-82

Google Scholar: [Author Only](#) [Title Only](#) [Author and Title](#)

Yang Z (2007) PAML 4: phylogenetic analysis by maximum likelihood. *Mol Biol Evol* 24: 1586-1591

Google Scholar: [Author Only](#) [Title Only](#) [Author and Title](#)

Zhang C, Dong SS, Xu JY, He WM, Yang TL (2019) PopLDdecay: a fast and effective tool for linkage disequilibrium decay analysis based on variant call format files. *Bioinformatics* 35: 1786-1788

Google Scholar: [Author Only](#) [Title Only](#) [Author and Title](#)